catalysts

MDPI

*Article*

# PTCL1-EstA from *Paenarthrobacter aurescens* TC1, a Candidate for Industrial Application Belonging to the VIII Esterase Family

**Qinyu Li [1,2,3], Xiaojia Chen [1,2,3], Xiangcen Liu [1,3], Zheng Chen [4], Yang Han [5], Peng Zhou [4], Jiping Shi [1,2,*] and Zhijun Zhao [1,*]**

1 Lab of Biorefinery, Shanghai Advanced Research Institute, Chinese Academy of Sciences, No. 99 Haike Road, Shanghai 201210, China; liqy@shanghaitech.edu.cn (Q.L.); chenxj@shanghaitech.edu.cn (X.C.); liuxiangcen2019@sari.ac.cn (X.L.)
2 School of Life Science and Technology, ShanghaiTech University, Shanghai 201210, China
3 University of Chinese Academy of Sciences, Beijing 100049, China
4 School of Health Science and Engineering, University of Shanghai for Science and Technology, Shanghai 200093, China; 201570146@st.usst.edu.cn (Z.C.); 211310154@st.usst.edu.cn (P.Z.)
5 School of Forestry, Northeast Forestry University, Harbin 150040, China; hanyang0163@163.com
* Correspondence: shijp@sari.ac.cn (J.S.); zhaozj@sari.ac.cn (Z.Z.); Tel.: +86-138-1763-8015 (J.S.); +86-180-1628-6015 (Z.Z.)

**Abstract:** The esterase PTCL1-EstA from *Paenarthrobacter aurescens* TC1 was expressed in *Escherichia coli* and characterized. An 1152 bp open reading frame encoding a 383 amino acid polypeptide was successfully expressed, the C-terminally His6-tagged PTCL1-EstA enzyme was purified, and the predicted molecular mass of the purified PTCL1-EstA was 40.6 kDa. The EstA family serine hydrolase PTCL1-EstA belongs to the esterase family VIII, contains esterase-labeled S-C-S-K sequences, and homologous class C beta-lactamase sequences. PTCL1-EstA favored p-nitrophenyl esters with C2-C6 chain lengths, but it was also able to hydrolyze long-chain p-nitrophenyl esters. Homology modelling and substrate docking predicted that Ser59 was an active site residue in PTCL1-EstA, as well as Tyr148, Ala325, and Asp323, which are critical in catalyzing the enzymatic reaction of p-nitrophenyl esters. PTCL1-EstA reached the highest specific activity against p-nitrophenyl butyrate (C4) at pH 7.0 and 45 °C but revealed better thermal stability at 40 °C and maintained high relative enzymatic activity and stability at pH 5.0–9.0. Fermentation medium optimization for PTCL1-EstA increased the enzyme activity to 510.76 U/mL, tapping the potential of PTCL1-EstA for industrial production.

**Keywords:** esterase; EstA family serine hydrolase; *Paenarthrobacter aurescens* TC1; heterologous expression



**Citation:** Li, Q.; Chen, X.; Liu, X.; Chen, Z.; Han, Y.; Zhou, P.; Shi, J.; Zhao, Z. PTCL1-EstA from *Paenarthrobacter aurescens* TC1, a Candidate for Industrial Application Belonging to the VIII Esterase Family. *Catalysts* **2022**, *12*, 473. https://doi.org/10.3390/catal12050473

Academic Editors: Edinson Yara-Varón and Ramon Canela-Garayoa

Received: 2 March 2022
Accepted: 19 April 2022
Published: 23 April 2022



## 1. Introduction

Lipolytic enzymes, including lipases, esterases (EC 3.1.1.1), triacylglycerol hydrolases, and carboxylester hydrolases, are among the most important biocatalysts and have a myriad of industrial and biotechnological applications [1], such as in the food and paper industries, biodiesel fuel production, detergent additive field, synthesis of fine chemicals and optically pure compounds, pesticide degradation in wastewater treatment, etc. [2,3]. One of the best-known esterases used in industry is *Candida antarctica* lipase B (CalB), which is derived from fungi [4,5]. Due to its high activity and stability under both aqueous and nonaqueous conditions, and the fact that it has a very wide range of substrate specificities, CalB has been used to catalyze the synthesis of esters, for instance, flavor and fragrance compounds and biodiesel [6,7].

Based on a comparison of the amino acid sequences and some fundamental biological properties, bacterial esterases and lipases were classified into eight different families [8]. In most esterases and lipases, a minimal conserved consensus sequence around the active site serine residue is located at the center of the conserved pentapeptide sequence motif

Gly-X-Ser-X-Gly or GDSL [9,10]. In addition, Evamaria I. Petersen et al. identified a novel esterolytic enzyme that contained an S-X-X-K motif, which exhibited sequence homology to α/β-lactamase [11]. In both of these highly homologous sequences, serine residues were predicted to be the active site for the esterase, which led to the classification of it as a serine hydrolase. A comparison of the amino acid sequences and structures of serine hydrolases indicates that the active site of these enzymes consists of a catalytic triad formed by Ser, His, and Asp or Glu and shows a high degree of homology to class C β-lactamases, which are classified as family VIII and share a common SXXK sequence [12–14].

Esterases and lipases are classified into two categories based on their substrate specificity for p-nitrophenol acyl esters [14]. These lipolytic enzymes all belong to the α/β-hydrolase structural superfamily and exhibit a common parallel β chain surrounded by α-helix connections in the tertiary structure. Esterases hydrolyze the ester bonds of water-soluble acyl esters with short-chain acyl groups (≤C8) and emulsified glycerides, while lipases prefer water-insoluble acyl esters and emulsified substrates with long-chain acyl groups (≥C10) [15,16].

In general, esterases (EC 3.1.1.1) can be useful biocatalysts as some show a certain substrate specificity, enantioselectivity, ability to sustain activity in organic solvents, and high product yields [12,14]. Due to their high industrial potential, these enzymes reveal special significance in various biotechnological applications, and the search for enzymes with novel properties is accelerating [17]. Despite the publication of several articles describing the cloning and expression of microbial esterases [18–21], to achieve the optimal performance of esterases in the industrial field, finding esterases with excellent thermal stability, stability in organic solvent environments, and a more diverse substrate selectivity is the main purpose of bioprospecting [22].

Most lipases investigated are from bacterial sources, such as enzymes from the genera *Bacillus*, *Pseudomonas*, *Geobacillus*, *Streptomyces*, *Achromobacter*, *Burkholderia*, *Chromobacterium*, *Arthrobacter*, and *Alcaligenes* [2]. Microorganisms that grow in environments with extreme pH, salinity, and temperature conditions are also important sources of lipases with industrial potential [23]. *Paenarthrobacter aurescens* TC1 (formerly *Arthrobacter aurescens* TC1) is a high G+C content Gram-positive aerobic bacterium that acts as a bacterial bioremediate to degrade the herbicide atrazine and has been shown to degrade most other common amino acids [24–26]. Due to the presence of duplicated catabolic genes and its ability to funnel plasmid-derived intermediates into chromosomally encoded pathways, the *P. aurescens* strain can survive and prosper under various pressure and temperature conditions [27].

In this paper, we describe the cloning, functional expression in *Escherichia coli*, purification, and characterization of an EstA family serine hydrolase PTCL1-EstA from *P. aurescens TC1*, and through fermentation optimization, we show that the enzyme activity is greatly improved.

## 2. Results and Discussion

### *2.1. Gene Cloning and Sequence Analysis*

A BLAST search (http://blast.ncbi.nlm.nih.gov/Blast.cgi, accessed on 2 March 2022) with the *PTCL1-EstA* gene sequence indicated that the *PTCL1-EstA* gene had an open reading frame of 1152 bp, encoded a polypeptide of 383 amino acid residues, had a predicted molecular mass of 40,681.98 Da, and had a calculated isoelectric point of pH 5.12.

The enzyme PTCL1-EstA characterized in this paper showed the highest similarity (98%) to the EstA family serine hydrolases from *Paenarthrobacter aurescens* (WP_011776415.1), which is consistent with the results of the putative gene sequence. Figure 1a shows the sequence alignment analysis of the PTCL1-EstA from *P. aurescens TC1*, EstA family serine hydrolase (WP_011776415.1) from *Paenarthrobacter aurescens*, CubicO group peptidase (MBP2268643.1) from *Pseudarthrobacter* sp. PvP004, EstA family serine hydrolase (WP_024818486.1) from *Arthrobacter* sp. 31Y, beta-lactamase family protein (UKA49595.1) from *Arthrobacter* sp. FW305-123, EstA family serine hydrolase (WP_026542666.1) from *Paenarthrobacter nicotinovorans*, serine hydrolase (WP_189020767.1) from *Paenarthrobacter*

*histidinolovorans*, serine hydrolase (WP_217376917.1) from *Paenarthrobacter ureafaciens*, EstA family serine hydrolase (WP_028267693.1) from *Arthrobacter* sp. MA-N2, serine hydrolase (WP_120520259.1) from *Arthrobacter celericrescens*, serine hydrolase (WP_058932481.1) from *Pseudarthrobacter sulfonivorans*, and serine hydrolase (WP_188729720.1) from *Pseudarthrobacter scleromae*. A phylogenetic tree was subsequently constructed using MEGA X software (Figure 1b) to reveal evolutionary relationships. Through distance methods in MEGA X, a pairwise evolutionary distance was computed for all protein sequences to be studied, and a phylogenetic tree was constructed by the neighbor-joining method [28].

Comparison of the amino acid sequences of PTCL1-EstA revealed that the characteristic G-X-S-X-G sequence of esterases could not be found in the above amino acid sequence, nor did it contain the conserved G-D-S-L sequence specific to class II esterase proteins [29]. Nevertheless, the conserved S-C-S-K sequence upstream of this sequence and its high homology with the class C β-lactamase pattern suggest that PTCL1-EstA was an EstA family serine hydrolase.

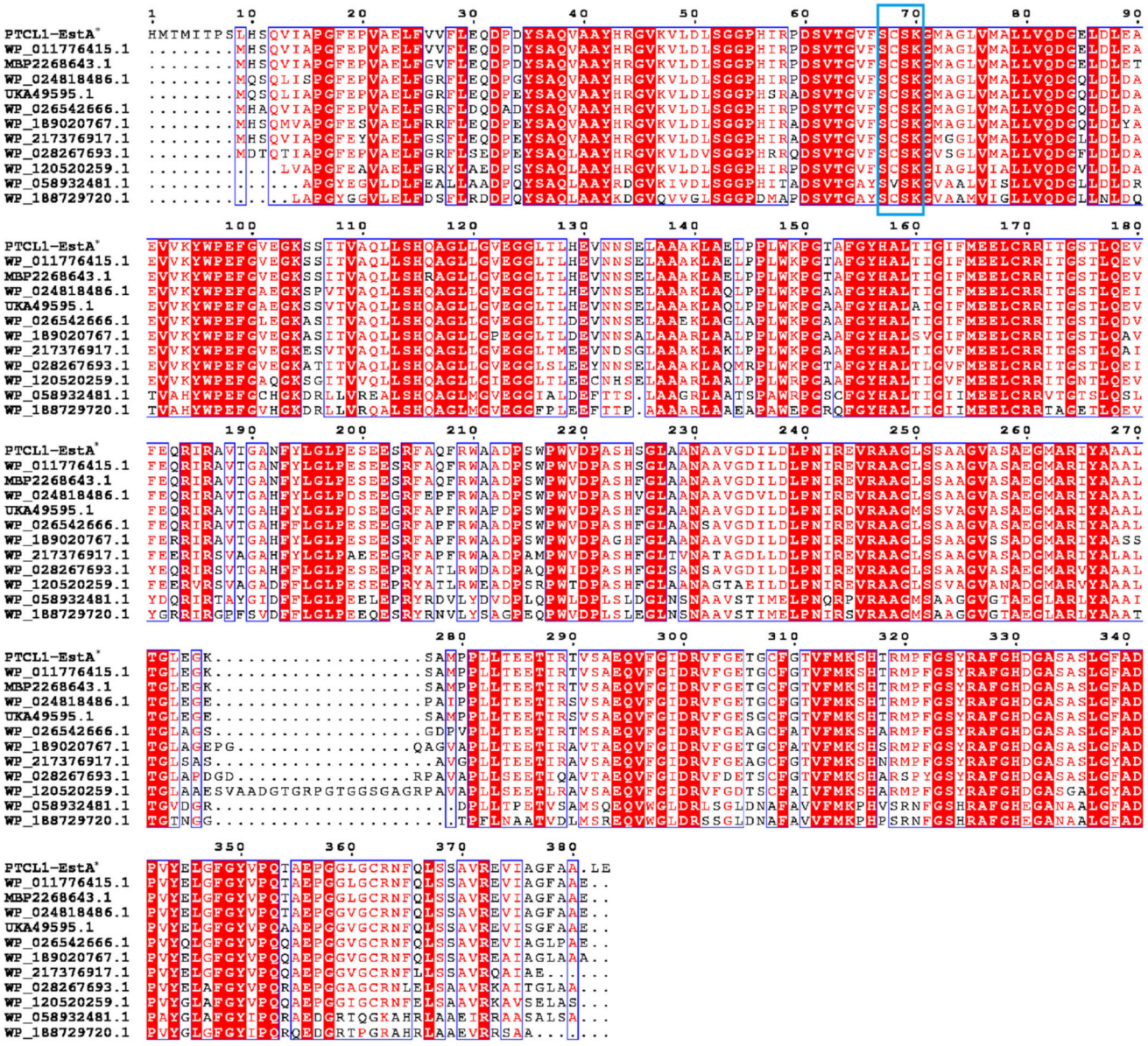


(**a**)

**Figure 1.** *Cont.*

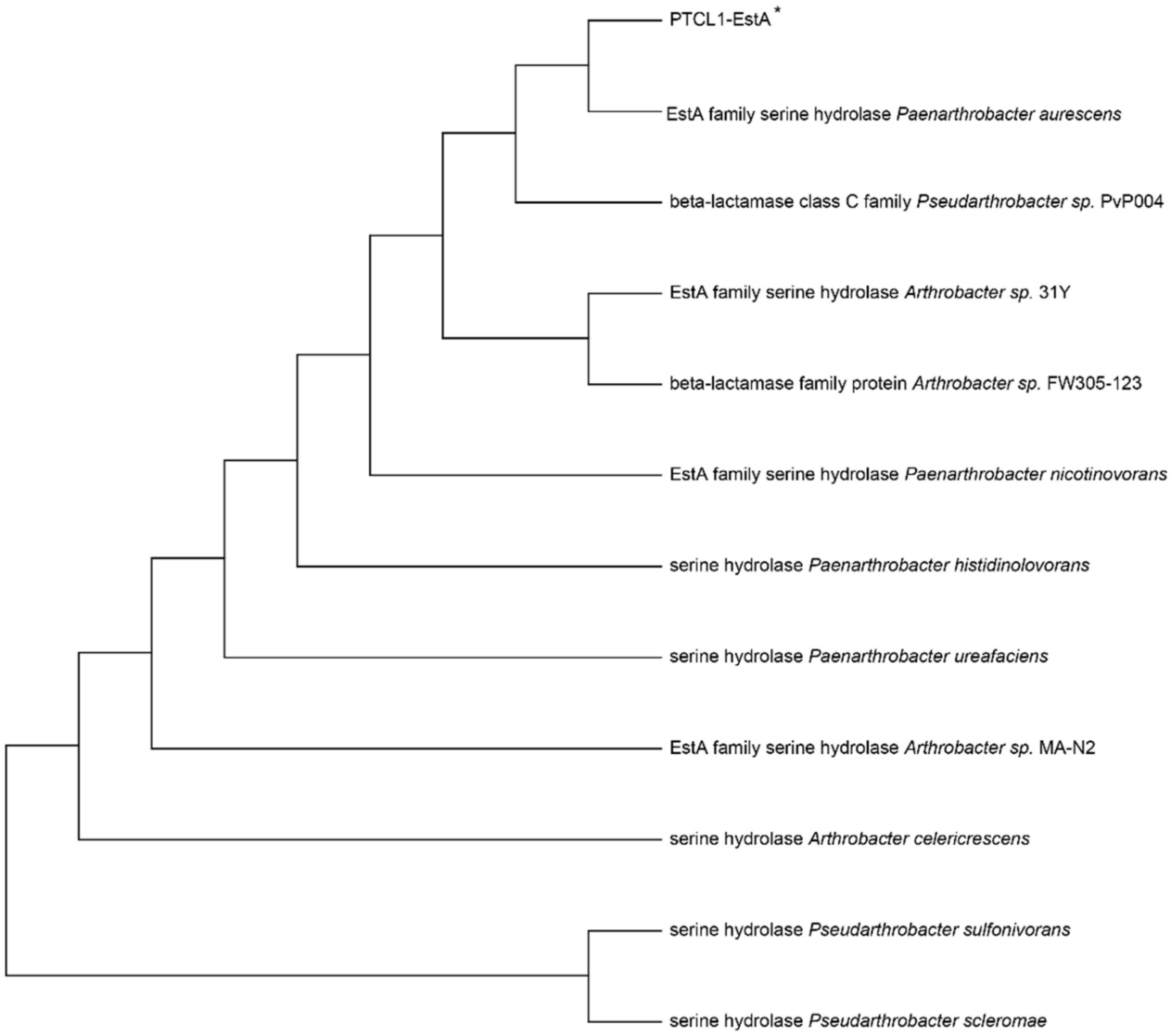


(**b**)

**Figure 1.** (**a**) Sequence alignment analysis of serine hydrolases from different species; (**b**) Phylogenetic tree of serine hydrolases from different species. The numbers below the lines represent the evolutionary distance. PTCL1-EstA is marked with "*".

The *PTCL1-EstA* gene was directly cloned into the pMD19-T vector for heterologous expression in *E. coli*. The obtained recombinant plasmid pMD19-EstA was propagated in *E. coli* DH5a and sequenced. The transformed strain was named DH5a-EstA. The plasmids with the correct sequence were used to transform into the *E. coli* BL21. The transformed strains were named BL21-EstA.

To purify the protein expressed from the *PTCL1-EstA* gene, we cloned the *PTCL1-EstA* gene into the plasmid pET28a, and we confirmed that the esterase gene was inserted successfully into the frame with the sequence encoding the His6-tag. The obtained recombinant plasmid pET28a-EstA was also propagated in *E. coli* DH5a, sequenced, and then transformed into *E. coli* BL21. The transformed strain with the plasmid pET28a-EstA was named BL21-His6EstA.

### *2.2. Enzymatic Properties of PTCL1-EstA*

The His6-tagged PTCL1-EstA was purified from a shake flask culture of *E. coli* BL21-His6EstA after 36 h of cultivation. As determined by SDS–PAGE, the purified PTCL1-EstA

was consistent with the predicted molecular weight (40.6 kDa). As shown in Figure 2a, a major specific protein band was obtained after purification.

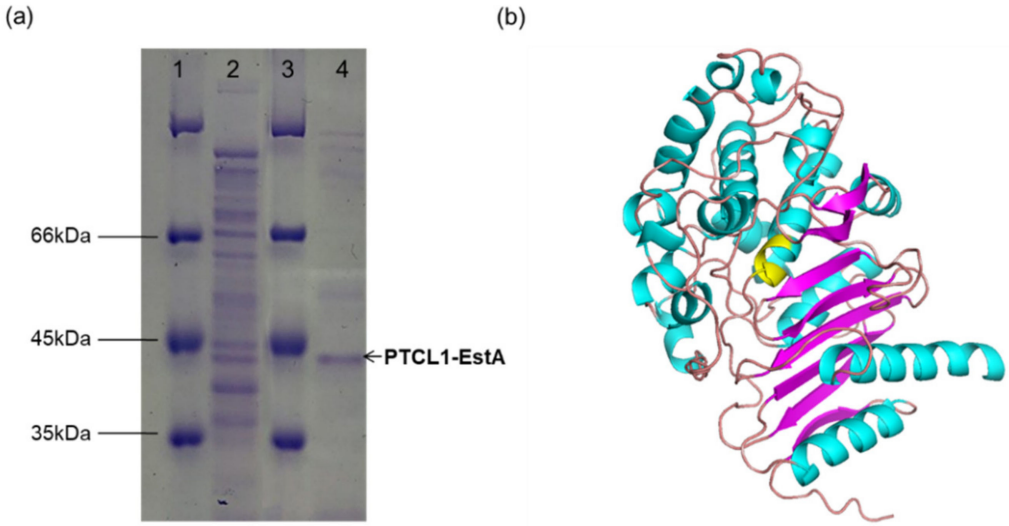


**Figure 2.** (**a**) SDS–PAGE image of purified PTCL1-EstA expressed in *E. coli*. Lanes 1 and 3: protein marker; lane 2: crude enzyme solution; lane 4: purified PTCL1-EstA. (**b**) The homology structural model of PTCL1-EstA. The residues in yellow indicate the putative active site.

A validated web-server-based protein modelling program (Swiss-Model) was used to construct a structural model of PTCL1-EstA. The complete protein sequence of PTCL1-EstA was submitted to the webserver, and the homologous protein structure of PTCL1-EstA (QMEAN value: −1.30) constructed by the program was evaluated using the evaluation statistics available on the website. The most pronounced homology was obtained for esterase A from *Arthrobacter nitroguajacolicus* Rü61a [30] (PDB ID: 3zyt.1; GMQE value: 0.82), esterase A from *Caulobacter crescentus* [31] (PDB ID: 5gkv.1; GMQE value: 0.68) and beta-lactamase from *Chromobacterium violaceum* [32] (PDB ID: 5evl.1; GMQE value: 0.63). Both esterase A and PTCL1-EstA are from the genus *Arthrobacter*, with >98% protein sequence similarity. These two proteins differ in amino acid residues at Val27, Gln116, Ser225, and Leu360 but share homologous S-C-S-K active site serines, similar to C-like β-lactamases, which are presumed to have very similar secondary structures [33]. Since esterase A from *Arthrobacter nitroguajacolicus* Rü61a can catalyze the hydrolysis of carboxylic acid esters and short-chain triglycerides, it was judged to belong to the lipase/esterase family VIII [11]. Thus, PTCL1-EstA was determined to belong to the lipase/esterase family VIII. The homology model of PTCL1-EstA is shown in Figure 2b. Like other family VIII esterase structures, the structure of PTCL1-EstA is composed of two domains, including a central α/β domain and a domain consisting of helices and loops [12]. The α/β domains are both composed of three antiparallel β-sheets.

We measured the substrate specificity of PTCL1-EstA by selecting p-nitrophenyl esters of different chain lengths as substrates. The purified His6-tagged PTCL1-EstA revealed a quite different preference for p-nitrophenyl esters than other esterases. In contrast to the FTT0941c esterase from *Francisella tularensis* which showed the lowest activity in the catalysis of p-nitrophenyl butyrate (C4) [34], PTCL1-EstA showed the highest activity in the hydrolysis of p-nitrophenyl butyrate (C4). As shown in Figure 3a, we evaluated the enzymatic specific activity of PTCL1-EstA on p-nitrophenyl esters of different chain lengths at pH 7.0 and 40 °C. With p-nitrophenyl butyrate (C4) as substrate, the enzyme specific activity value was 144.07 U/mg, which was set at 100%. Purified PTCL1-EstA had a typical hydrolytic preference for short-chain p-nitrophenyl esters, with the significant hydrolytic ability for p-nitrophenyl acetate (C2) and p-nitrophenyl hexanoate (C6), reaching relative hydrolytic activities of 79.29% and 89.024%, respectively. The purified PTCL1-EstA

also showed moderate hydrolytic ability towards p-nitrophenyl esters with medium to long carbon chains. For example, the relative activities for p-nitrophenyl octanoate (C8) and p-nitrophenyl laurate (C12) were 47.865% and 48.081%, respectively. However, the hydrolysis of long-chain p-nitrophenyl palmitate (C16) was not significant, with a relative activity of only 13.47%.

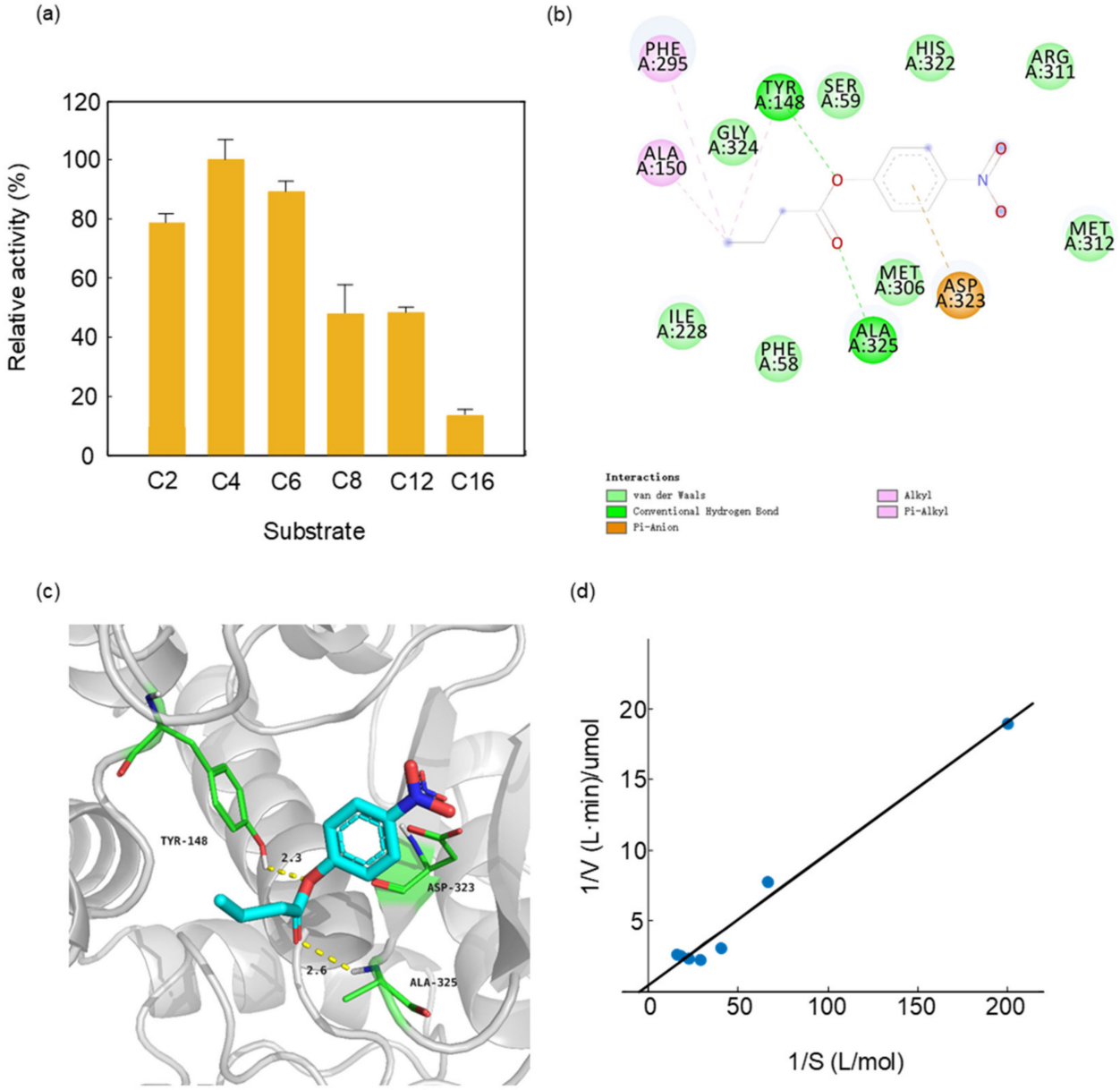


**Figure 3.** (**a**) Substrate specificity of PTCL1-EstA; (**b**) 2D ligand interaction diagram of PTCL1-EstA with a docked p-nitrophenyl butyrate (C4); (**c**) active site of PTCL1-EstA with a docked p-nitrophenyl butyrate (C4); (**d**) $K_m/V_{max}$ values of PTCL1-EstA.

A structural model of docking PTCL1-EstA with p-nitrophenyl butyrate (C4) was created to confirm the experimental results regarding substrate specificity. Docking was performed via the rigid receptor scheme in Discovery Studio 4.1 software based on the CHARMm docking tool CDOCKER. Structurally, p-nitrophenylbutyrate (C4) was stabilized in PTCL1-EstA by hydrogen bonds as well as hydrophobic interactions, as shown in Figure 3b. The crucial amino acid residues are shown with their respective numbers. The results of docking indicated that the nucleophilic serine and general bases in the catalytic triad of PTCL1-EstA were identified as Ser59, His322, and Asp323, respectively. In

addition, three different amino acids, Tyr148, Ala325, and Asp323, were chosen as potential catalytic members involved in the enzymatic mechanism and enhancing the enzymatic reaction (Figure 3c).

In order to demonstrate the wide range of industrial applications of PTCL1-EstA, three other substrates were chosen for molecular docking with a homologous model of PTCL1-EstA: the typical β-lactam antibiotics ampicillin, cephalothin, and a plasticizer dimethyl phthalate. Dimethyl phthalate is commonly used in the production of films, varnishes, transparent paper, etc. [35]. Due to its low volatility, dimethyl phthalate poses a strong ecological hazard and can cause gastrointestinal irritation, central nervous system depression and paralysis, and reduced blood pressure when accidentally ingested by humans [36]. We used Autodock vina software [36] to perform partial flexibility docking of these three substrates with PTCL1-EstA. Based on the docking results in Figure S1, we speculate that PTCL1-EstA is able to catalyze these three substrates. Ampicillin and cephalothin bind PTCL1-EstA through H bonds, while PTCL1-EstA and dimethyl phthalate form a stable steric structure through the hyperconjugation effect from C-H sigma orbitals and C-H alkyl orbitals. However, the electrostatic potential energy at docking was not high for them (Table S1), indicating that PTCL1-EstA could not bind them strongly. In general, the lower the value of the affinity, the closer the bond. These results are consistent with the highly homotypic enzyme Rue61a, which has specific enzymatic activities of only 0.1 U/mg for penicillin G and 0.2 U/mg for 6-aminopenicillins acid, respectively [31].

Figure 3d showed the $K_m$ and $V_{max}$ values of purified PTCL1-EstA, with 5, 15, 25, 35, and 45 mM p-nitrophenyl butyrate (C4) as the substrate. The concentration of p-nitrophenyl butyrate (C4) corresponding to the enzyme was measured at 40 °C for 15 min. The $K_m$ value of PTCL1-EstA for p-nitrophenyl butyrate (C4) was 60 mM, and the $V_{max}$ value was 20 U/mg, as determined by double reciprocal plotting.

The enzyme activity of PTCL1-EstA was measured by interactively activated titration with p-nitrophenyl butyrate (C4). Several pH values (3, 4, 5, 6, 7, 8, 9, 10, and 11) were applied to determine the effect of pH on the activity of PTCL1-EstA. The effect of pH on the enzyme specific activity of PTCL1-EstA is shown in Figure 4. Citrate-$Na_2HPO_4$ buffer and $Na_2CO_3$-$H_3BO_3$ buffer were used to achieve pH ranges of 3–8 and 7–11, respectively. PTCL1-EstA showed maximum enzyme activity at pH 7 with 144.07 U/mg. The enzyme specific activity of PTCL1-EstA at pH 7 was used as the standard (100%), and after incubation at 40 °C for 15 min at pH 5–7, PTCL1-EstA retained more than 40% relative activity, indicating its adaptability to weakly acidic environments (Figure 4a). The pH stability was characterized by measuring the residual relative activity at pH 7 after PTCL1-EstA had been incubated at different pH for a period of time. As shown in Figure 4b, PTCL1-EstA retained more than 60% of its relative activity after being left at pH 7 for 120 min. The enzyme relative activity continued to decrease with increasing incubation time at each pH. Even in the alkaline and acidic environments of pH 9 and pH 5, the enzyme relative activity of PTCL1-EstA was maintained at more than 40% after 120 min at 40 °C. In general, esterases of the VIII family are more tolerant of alkaline environments. However, PTCL1-EstA not only displayed excellent alkaline adaptability but also exhibited strong hydrolysis of p-nitrophenyl ester at acidic pH levels [3]. Under the incubation condition of pH 5, the relative activity of PTCL1-EstA revealed a fluctuating decrease with increasing incubation time until it completely lost its enzymatic activity at 300 min (data not shown). This result further indicates that PTCL1-EstA has high practical relevance in acidic industrial applications.

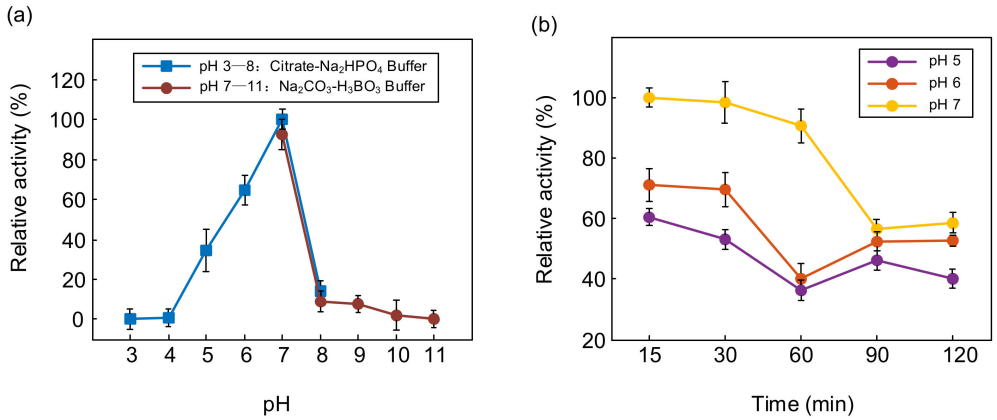


**Figure 4.** (**a**) Effect of pH on the relative activity of purified PTCL1-EstA; (**b**) pH stability of purified PTCL1-EstA.

The optimum temperature for PTCL1-EstA to hydrolyze p-nitrophenyl butyrate (C4) was determined to be from 25 °C to 70 °C. The relative activities of PTCL1-EstA at different temperatures are shown in Figure 5a. The enzymatic activity of PTCL1-EstA treated at 40 °C, pH 7, for 15 min was set as 100%. Similar to the reported esterases cloned from high-temperature-tolerant strains, PTCL1-EstA showed high-temperature tolerance, and maintained more than 50% relative activity even at incubation at 70 °C [30,35]. Between 37 °C and 45 °C, the relative enzyme activity of PTCL1-EstA was maintained more than 80%. The highest enzymatic activity of PTCL1-EstA was observed at 45 °C with 185.14 U/mg. The thermal stability of the enzyme PTCL1-EstA is shown in Figure 5b. The residual enzyme specific activity was measured after incubation at 40 °C and 45 °C for 5, 15, 30, 45, 60, and 120 min. Although PTCL1-EstA showed stronger enzyme specific activity at 45 °C for 15 min, there was a significant reduction after 30 min with the extension of the incubation time at 45 °C, and only 55.163% relative activity remained, and the relative activity decreased to 36.917% after 45 min. In contrast, with 60 min of incubation at 40 °C, the relative activity showed a slight fluctuation, and after 120 min of incubation, PTCL1-EstA still retained approximately 40% of its relative enzyme activity, indicating that PTCL1-EstA has better thermal stability at 40 °C.

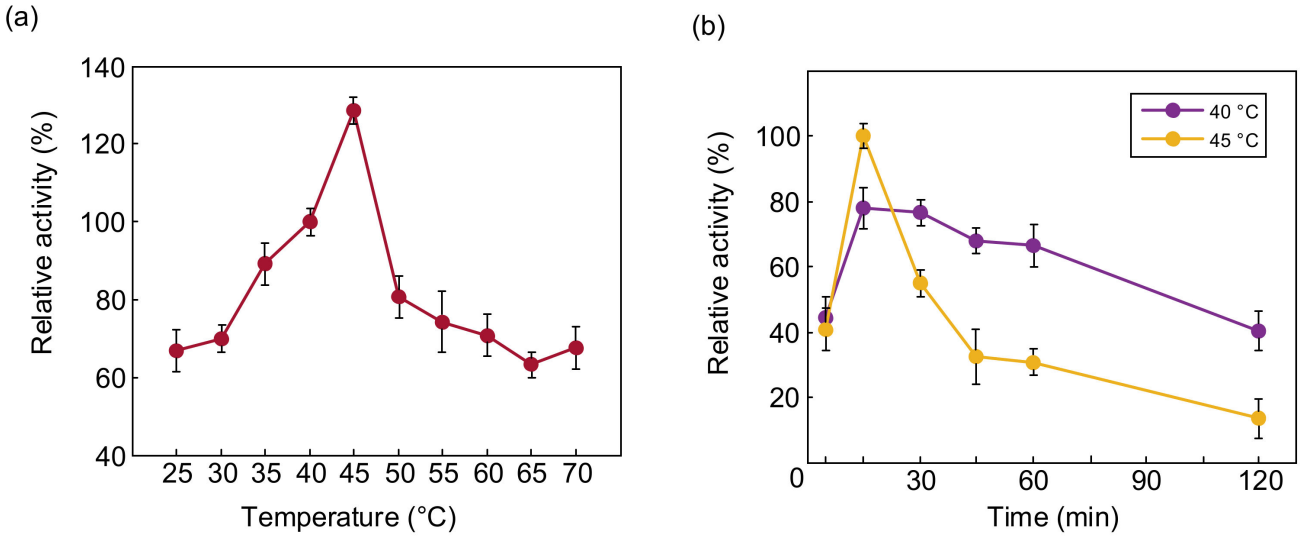


**Figure 5.** (**a**) Effect of temperature on the relative activity of purified PTCL1-EstA; (**b**) effect of temperature on the stability of purified PTCL1-EstA.

### *2.3. Fermentation Optimization of Recombinant Bacteria*

As the most commonly used host for expressing heterologous proteins, *E. coli* exhibits the benefits of easy molecular manipulation, minimal cost, and rapid protein expression in a relatively short fermentation period [37]. Nevertheless, heterologous proteins are usually expressed intracellularly in *E. coli*, which in turn requires engaging in highly expensive downstream processes such as cell lysis and generalization of the target protein [38]. The economical production of industrial- or agricultural-based proteins is still a challenge and requires significant reductions in industrial production costs [39]. Hence, we optimized the fermentation based on LB medium to improve the enzyme activity of *E. coli* BL21-EstA-produced PTCL1-EstA.

The effects of different types and concentrations of carbon and nitrogen sources on the growth intensity and PTCL1-EstA production of *E. coli* BL21-EstA are shown in Figure 6. We utilized four types of carbon sources, glycerol, glucose, sucrose, and maltodextrin, to explore the effects of carbon source types and concentrations on the growth intensity and enzyme production of *E. coli* BL21-EstA, as shown in Figure 6a,b. Different types of carbon sources had different effects on the growth intensity of *E. coli* BL21-EstA, and the $OD_{600}$ values after 36 h of shake flask cultivation were used to reflect the growth intensity of *E. coli* BL21-EstA. The highest growth intensity of *E. coli* BL21-EstA was achieved when malt dextrin was used as the carbon source; the $OD_{600}$ value was 21.86. However, the increase in growth intensity was not necessarily accompanied by an increase in enzyme production capacity, and the enzyme activity was only 31.02 U/mL under the medium with malt dextrin as the carbon source, which ranked last among the four carbon source optimization types. Throughout the carbon source optimization results, glycerol should be the optimal carbon source option. In the medium composition with glycerol as the carbon source, *E. coli* BL21-EstA not only reached the highest growth level of 14.19 $OD_{600}$ value but also produced the highest amount of enzyme activity, with 236.94 U/mL. Thus, glycerol was selected as the main carbon source for the fermentation medium. In Figure 6b, the specific ratio of glycerol addition to the medium was optimized, and 5 g/L glycerol was added to the medium as the optimal concentration. Under this cultivation condition, the $OD_{600}$ of *E. coli* BL21-EstA reached 18.043, and the enzyme activity of PTCL1-EstA increased to 312.05 U/mL.

Based on the optimization of the carbon source, we further optimized the nitrogen source composition of the medium. The following seven commonly used nitrogen sources were selected for the optimization of nitrogen source types: $(NH_4)_2SO_4$, $NH_4Cl$, $NH_4H_2PO_4$, $H_2NCONH_2$, $NaNO_3$, corn steep liquor powder, and soybean meal powder. As shown in Figure 6c, through the comprehensive comparison of the growth intensity and enzyme production capacity of *E. coli* BL21-EstA after 36 h cultivation in different nitrogen source media, $NaNO_3$ should be the best choice of nitrogen source. In the medium with $NaNO_3$ as the main nitrogen source, the $OD_{600}$ of *E. coli* BL21-EstA reached 18.342, and the PTCL1-EstA enzyme activity reached 347.16 U/mL. The optimization of the addition ratio of $NaNO_3$ in the medium showed that 5 g/L $NaNO_3$ in the medium was the best addition concentration (Figure 6d). After optimization, the $OD_{600}$ of *E. coli* BL21-EstA reached 18.45, and the PTCL1-EstA enzyme activity reached 366.96 U/mL.

The experimental results showed that PTCL1-EstA reached the highest enzyme activity under the medium conditions of 5 g/L glycerol, 5 g/L sodium nitrate, 18 g/L peptones, 24 g/L yeast powder, 2.31 g/L potassium dihydrogen phosphate, and 16.43 g/L dipotassium hydrogen phosphate. Based on this, we further optimized the fermentation temperature and the initial pH of the medium. The optimal fermentation temperature was 25 °C, and the optimal initial pH of the medium was 7.1. After optimization, the growth intensity of *E. coli* BL21-EstA was significantly increased (Figure S2). Finally, the enzyme activity of PTCL1-EstA was increased to 510.76 U/mL by optimizing the cultivation conditions, medium formulation, and the ratio of nitrogen and carbon sources in the shake flask cultivation for 36 h, which is the highest enzyme activity among the reported VIII esterase family of enzymes.

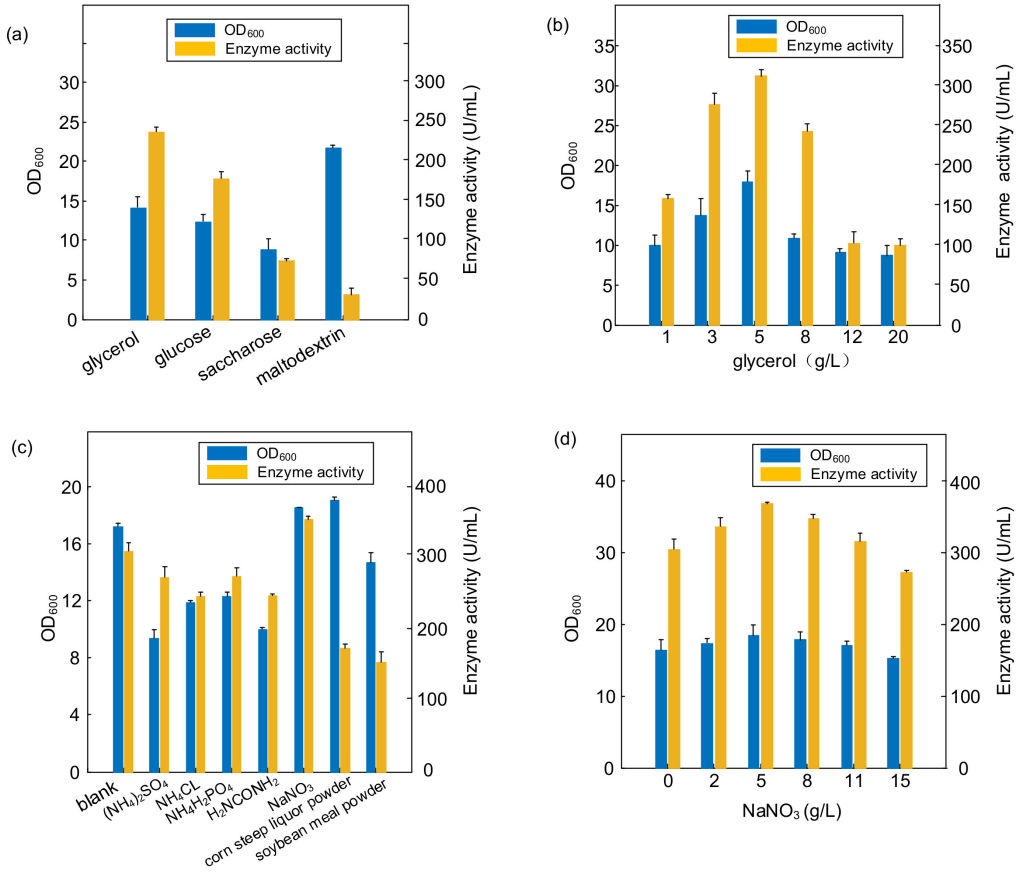


**Figure 6.** (**a**) Effect of different carbon substrates; (**b**) effect of the ratio of glycerol addition; (**c**) effect of different nitrogen substrates; (**d**) effect of the ratio of $NaNO_3$ addition.

## 3. Materials and Methods

### *3.1. Bacterial Strains and Plasmids*

The hosts for plasmid transformation and expression were the *E. coli* strains DH5α and BL21. The *P. aurescens* TC1 strain and empty plasmid pET28a were stored in the laboratory. The Taq DNA polymerase, restriction endonuclease, genome extraction kit, plasmid extraction kit, molecular purification kit, and pMD19-T simple vector were purchased from Takara (Dalian, China). Recombinant plasmids were constructed by using the ClonExpress® II One-Step Cloning Kit, which was purchased from Vazyme Biotech Co., Ltd. (Nanjing, China). Primers were synthesized by Sangon Biological Engineering Technology and Services (Shanghai, China).

### *3.2. Gene Cloning and Expression Vector Construction*

A homology search of the GenBank database was performed by the BLAST program (http://blast.ncbi.nlm.nih.gov/Blast.cgi, accessed on 2 March 2022), and multiple alignments were carried out by using the DNAMAN program. A phylogenetic tree of homologous serine hydrolase and esterase proteins was constructed using the neighbor-joining algorithm in MEGA X software. Through distance methods in MEGA X, a pairwise evolutionary distance was computed for all protein sequences to be studied, and a phylogenetic tree was constructed by the neighbor-joining method.

Genomic DNA of *P. aurescens* TC1 was prepared by the reported method [31–33]. The primers PTCL1-EstA For and PTCL1-EstA Rev were designed based on the putative AAAA_RS19005 gene (NCBI gene ID: 29622418) of *P. aurescens* TC1 (AABI_ classification ID: 290340) to obtain the gene fragment PTCL1-EstA. Polymerase chain reaction (PCR) amplification was performed using PrimeSTAR DNA polymerase. The PCR amplification program was initiated at 94 °C for 5 min, with 35 cycles of 94 °C for 30 s, 54 °C for 1 min,

72 °C for 30 s, and a final extension of 72 °C for 10 min. The amplified product obtained after isolating the PCR product was ligated into the pMD19-T simple vector with an In-Fusion cloning kit to generate the recombinant plasmid. After gene sequencing, the target recombinant plasmid was successfully constructed. These plasmids were transformed into the *E. coli* DH5α strain and stored. The plasmid with the correct sequence was finally transformed into chemically competent *E. coli* BL21 cells. The transformed strain was named BL21-EstA.

Similarly, the recombinant plasmid pET28a-EstA was constructed using the In-Fusion cloning kit by obtaining the target fragments from the genome using primers pET28a-EstA For and pET28a-EstA Rev. The recombinant plasmid was propagated in *E. coli* DH5a for sequencing and then transformed into *E. coli* BL21. The strain was named BL21-His6EstA and used to obtain the pure PTCL1-EstA enzyme. Table 1 shows the primers used in this study.

**Table 1.** Primers used in this study.

| Primer | Sequence (5′–3′) |
|---|---|
| PTCL1-EstA For | (5′-CGCGCGGATCTTCCAGAGATATGGCGGCCGGAGT-3′) |
| PTCL1-EstA Rev | (5′-CACGCCTGCCGTTCGACGATCCGCCCGGATTCAGTCAC-3′) |
| pET28a-EstA For | (5′-CTCGAGTGCGGCCGCAAGCTATGGCGGCCGGAGTCCC-3′) |
| pET28a-EstA Rev | (5′-GGGTCGCGGATCCGAATTTCCGCCCGGATTCATCACCG-3′) |

### *3.3. Homology Protein Structure Modelling*

A validated web-server-based protein modelling program (Swiss-Model) was used to construct a structural model of PTCL1-EstA. The complete protein sequence of PTCL1-EstA was submitted to the webserver (https://swissmodel.expasy.org/, accessed on 2 March 2022). The homology protein structure of PTCL1-EstA constructed by the program was evaluated using the evaluation statistics available on the website. The PTCL1-EstA structure diagram was constructed and modified in PyMOL software.

Docking was performed via the rigid receptor scheme in Discovery Studio 4.1 software based on the CHARMm docking tool CDOCKER.

### *3.4. Growth Media and Conditions*

The *P. aurescens* TC1 strain was grown aerobically in a medium containing 10 g/L peptones, 5 g/L glucose, 5 g/L yeast extract, 5 g/L NaCl and 2.5 g/L $MgSO_4.7H_2O$, pH 7.0, at 37 °C, collected and stored at −80 °C in retention tubes with 15% glycerol [40–42].

*E. coli* was cultured using LB seed medium (5 g/L yeast extract, NaCl 10 g/L, 10 g/L peptones, pH 7.1, sterilized at 121 °C for 20 min). The initial formulation of reconstituted *E. coli* shake flask fermentation medium was 12 g/L peptone, 8 g/L glucose, 24 g/L yeast extract, 12.54 g/L $K_2HPO_4$ and 2.31 g/L $KH_2PO_4$. In this paper, we optimized the carbon and nitrogen sources based on this medium formulation. Furthermore, the fermentation process was optimized based on the optimal initial pH and cultivation temperature.

For the shake flask fermentation of *E. coli* BL21-EstA, the seed solution was inserted into a 250 mL shake flask with 50 mL of fermentation medium, the inoculum volume was 2.5 mL (5% *v*/*v*), and the culture was shaken for 36 h at 37 °C and 200 rpm in a rotary shaker.

The $OD_{600}$ value determination for *E. coli* was conducted as follows: one milliliter of fermentation broth was centrifuged at 12,000 rpm for 2.5 min, and then the supernatant was discarded. The bacterium was washed 1–2 times after redissolution with distilled water and then resuspended with distilled water to determine the bacterial density $OD_{600}$ with distilled water as the blank. If the spectrophotometer reading was within the range of producing large errors, the bacterial broth was diluted appropriately to achieve an $OD_{600}$ of 0.2~0.8. The data were expressed as the average of three samples.

### *3.5. Protein Purification*

The fermentation broth was sampled at the end of the shake flask fermentation, and the obtained samples were centrifuged at 12,000 rpm for 2 min to collect the bacterial cells. The collected cells were resuspended in 20 mM/L pipera-zine-1,4-diethanesulfonic acids (PIPES) buffer. Then, the recombinant *E. coli* cells were crushed by an ultrasonic solicitor (model: Scientz-11D, Ningbo Scientz Biotechnology Co., Ltd., Ningbo, China). The total crushing time was 10 min; the crushed solution was centrifuged at 5 °C and 12,000 rpm for 6 min, and the supernatant was collected to prepare a crude enzyme solution. The PTCL1-EstA crude enzyme solution was subjected to Ni-affinity chromatography using a Ni-TED 5 mL Sefinose™ column (Sangon Biotech, Shanghai, China). 6xHis-labelled PTCL1-EstA was eluted with a linear gradient of elution buffer (500 mM PBS/pH 7.0 containing 500 mM imidazole and 300 mM NaCl). The concentration of protein was measured according to the Bradford method [43].

### *3.6. Enzyme Activity Assay*

PTCL1-EstA hydrolyses p-nitrophenyl butyrate (C4) to p-nitrophenol, which has a maximum absorption peak at 410 nm [44]. The absorbance value at 410 nm of PTCL1-EstA was used as the enzymatic activity index for enzymatic activity measurements [34].

The reaction system for enzyme activity determination was as follows: a total of 1 mL of substrate buffer (p-nitrophenyl butyrate solution) was added to a 5 mL EP tube and incubated at 40 ± 0.5 °C for 15 min, 50 µL of enzyme solution was added, the mixture was placed at 40 ± 0.5 °C for 15 min, 2.0 mL of acetone was added, and the mixture was stirred thoroughly to terminate the reaction. The absorbance of the reaction system was analyzed at 410 nm. The amount of enzyme required to produce 1 mM of p-nitrophenol in 1 min was defined as a standard unit of enzyme activity (U) Three samples were conducted, and data were expressed as an average.

## 4. Conclusions

An EstA family serine hydrolase gene (*PTCL1-EstA*) was cloned and expressed from a *P. aurescens* TC1 gene library. This is the first report to demonstrate the cloning, expression, purification, and characterization of an esterase from *P. aurescens* TC1. The substrate ranges of PTCL1-EstA favored p-nitrophenyl esters with a chain length of C2–C6, and the enzyme had the ability to hydrolyze long-chain p-nitrophenyl esters. Homology modelling and substrate docking suggested that Ser59 was an active site residue in PTCL1-EstA, as well as Tyr148, Ala325 and Asp323, which are critical in catalyzing the enzymatic reaction of p-nitrophenyl esters. Being derived from a high temperature- and pressure-tolerant strain, the recombinant PTCL1-EstA exhibited good stability at elevated temperatures and was active over a broad temperature and pH range. Following the optimization of PTCL1-EstA for carbon and nitrogen sources of fermentation medium, the enzymatic activity of PTCL1-EstA was effectively improved, tapping its potential for industrial large-scale production.

**Supplementary Materials:** The following supporting information can be downloaded at: https://www.mdpi.com/article/10.3390/catal12050473/s1, Table S1: The electrostatic potential energy of molecular docking, Figure S1: (a) Molecular docking of PTCL1-EstA with ampicillin; (b) molecular docking of PTCL1-EstA with cephalothin; (c) molecular docking of PTCL1-EstA with dimethyl phthalate, Figure S2: (a) Effect of cultivation temperature; (b) effect of initial pH of fermentation medium.

**Author Contributions:** Data analysis and writing, Q.L.; figures, X.C. and X.L.; data collection, Z.C.; literature search, Y.H.; data interpretation, P.Z. and J.S.; study design, Z.Z. All authors have read and agreed to the published version of the manuscript.

**Funding:** This research was funded by "Research and demonstration application of biocritical technology for low purine soy products", grant number: 21SH20.

**Acknowledgments:** We would like to thank Dr. Zhang Baoguo (Shanghai Advanced Research Institute, Chinese Academy of Sciences) for valuable suggestions on this manuscript.

**Conflicts of Interest:** The authors declare no conflict of interest.

## References

1. Pichapak, S.; Fusako, K.; Somjai, S.; Kosum, C.; Thayat, S. Cloning, Expression and Characterization of a Thermostable Esterase HydS14 from *Actinomadura* sp. Strain S14 in Pichia pastoris. *Int. J. Mol. Sci.* **2015**, *16*, 13579–13594.
2. Samoylova, Y.V.; Sorokina, K.N.; Piligaev, A.V.; Parmon, V.N. Application of Bacterial Thermostable Lipolytic Enzymes in the Modern Biotechnological Processes. *Catal. Ind.* **2019**, *11*, 168–178. [CrossRef]
3. Miguel-Ruano, V.; Rivera, I.; Rajkovic, J.; Knapik, K.; Torrado, A.; Otero, J.M.; Beneventi, E.; Becerra, M.; Sánchez-Costa, M.; Hidalgo, A.; et al. Biochemical and Structural Characterization of a novel thermophilic esterase EstD11 provide catalytic insights for the HSL family. *Comput. Struct. Biotechnol. J.* **2021**, *19*, 172–179. [CrossRef] [PubMed]
4. Chodorge, M.; Fourage, L.; Ullmann, C.; Duvivier, V.; Masson, J.M.; Synthesis, F.L.J.A. Rational Strategies for Directed Evolution of Biocatalysts—Application to *Candida antarctica* lipase B (CALB). *Catalysis* **2005**, *347*, 1022–1026.
5. Pan, Z.Y.; Yang, Z.M.; Pan, L.; Zheng, S.P.; Han, S.Y.; Lin, Y. Displaying *Candida antarctica* lipase B on the cell surface of *Aspergillus niger* as a potential food-grade whole-cell catalyst. *Biotechnology* **2014**, *41*, 711–720. [CrossRef] [PubMed]
6. Inaba, C.; Maekawa, K.; Morisaka, H. Efficient synthesis of enantiomeric ethyl lactate by *Candida antarctica* lipase B (CALB)-displaying yeasts. *Appl. Microbiol. Biotechnolo.* **2009**, *83*, 859–864. [CrossRef]
7. Seo, H.S.; Kim, S.E.; Han, K.Y.; Park, J.S.; Kim, Y.H.; Sang, J.S.; Lee, J. Functional fusion mutant of *Candida antarctica* lipase B (CalB) expressed in *Escherichia coli*. *Proteomics* **2009**, *1794*, 519–525. [CrossRef] [PubMed]
8. Syed, M.N.; Mohamad, A.M.; Abd, R.; Suriana, S.; Anuar, J.M.; Chor, L.T. Crystallization and structure elucidation of GDSL esterase of *Photobacterium* sp. J15. *Int. J. Biol. Macromol.* **2018**, *119*, 1188–1194.
9. Akoh, C.C.; Lee, G.C.; Liaw, Y.C.; Huang, T.H.; Shaw, J.F. GDSL family of serine esterases/lipases. *Prog. Lipid Res.* **2004**, *43*, 534–552. [CrossRef]
10. Arpigny, J.L.; Jaeger, K.E. Bacterial lipolytic enzymes: Classification and properties. *Biochem. J.* **1999**, *343*, 177–183. [CrossRef]
11. Shakiba, M.H.; Ali, M.S.; Rahman, R.N.; Salleh, A.B.; Leow, T.C. Cloning, expression and characterization of a novel cold-adapted GDSL family esterase from *Photobacterium* sp. strain J15. *Extremophiles* **2015**, *20*, 1–11. [CrossRef] [PubMed]
12. Nicolay, T.; Devleeschouwer, K.; Vanderleyden, J.; Spaepen, S. Characterization of Esterase A, a *Pseudomonas stutzeri* A15 Autotransporter. *Appl. Environ. Microbiol.* **2012**, *78*, 2533–2542. [CrossRef]
13. Petersen, E.I.; Valinger, G.; Sölkner, B.; Stubenrauch, G.; Schwab, H. A novel esterase from *Burkholderia gladioli* which shows high deacetylation activity on cephalosporins is related to β-lactamases and dd-peptidases. *J. Biotechnol.* **2001**, *89*, 11–25. [CrossRef]
14. Wagner, U.G.; Petersen, E.I.; Schwab, H.; Kratky, C.; Science, K.J.P. EstB from *Burkholderia gladioli*: A novel esterase with a beta-lactamase fold reveals steric factors to discriminate between esterolytic and beta-lactam cleaving activity. *Protein Sci.* **2010**, *11*, 467–478. [CrossRef] [PubMed]
15. Bornscheuer, U.T. Microbial carboxyl esterases: Classification, properties and application in biocatalysis. *Fems Microbiol. Rev.* **2002**, *26*, 73–81. [CrossRef]
16. Brod, F.C.A.; Vernal, J.; Bertoldo, J.B.; Terenzi, H.; Arisi, A.C.M. Cloning, Expression, Purification, and Characterization of a Novel Esterase from *Lactobacillus plantarum*. *Mol. Biotechnol.* **2010**, *44*, 242–249. [CrossRef] [PubMed]
17. Chiş, L.; Hriscu, M.; Bica, A.; Toşa, M.; Nagy, G.; Róna, G.; Vértessy, B.G.; Dan Irimie, F. Molecular cloning and characterization of a thermostable esterase/lipase produced by a novel *Anoxybacillus flavithermus* strain. *J. Gen. Appl. Microbiol.* **2013**, *59*, 119–134. [CrossRef] [PubMed]
18. Ewis, H.E.; Abdelal, A.T.; Lu, C.D. Molecular cloning and characterization of two thermostable carboxyl esterases from *Geobacillus stearothermophilus*. *Gene* **2004**, *329*, 187–195. [CrossRef]
19. Donaghy, J.; McKay, A.M. Purification and characterization of a feruloyl esterase from the fungus *Penicilliumexpansum*. *J. Appl. Microbiol.* **2003**, *83*, 718–726. [CrossRef]
20. Kaiser, P.; Raina, C.; Parshad, R.; Johri, S.; Verma, V.; Andrabi, K.I.; Qazi, G.N. A novel esterase from *Bacillus subtilis* (RRL 1789): Purification and characterization of the enzyme. *Protein Expr. Purif.* **2006**, *45*, 262–268. [CrossRef]
21. Wang, X.; Xin, G.; Egashira, Y.; Sanada, H. Purification and Characterization of a Feruloyl Esterase from the Intestinal Bacterium *Lactobacillus acidophilus*. *Appl. Environ. Microbiol.* **2004**, *70*, 2367–2372. [CrossRef] [PubMed]
22. Amaki, Y.; Edgard, E.T.; Ueda, S.; Ohmiya, K.; Yamane, T. Purification and Properties of a Thermostable Esterase of *Bacillus stearothermophilus* Produced by Recombinant *Bacillus brevis*. *Biosci. Biotechnol. Biochem.* **1992**, *56*, 238–241. [CrossRef]
23. Contesini, F.J.; Davano, M.G.; Borin, G.P.; Vanegas, K.G.; Carvalho, P.J.C. Advances in Recombinant Lipases: Production, Engineering, Immobilization and Application in the Pharmaceutical Industry. *Catalysts* **2020**, *10*, 1032. [CrossRef]
24. Samoylova, Y.V.; Sorokina, K.N.; Romanenko, M.V.; Parmon, V.N. Cloning, expression and characterization of the esterase estUT1 from *Ureibacillus thermosphaericus* which belongs to a new lipase family XVIII. *Extremophiles* **2018**, *22*, 271–285. [CrossRef] [PubMed]

25. Viegas, C.A.; Silva, V.P.; Varela, V.M. Evaluating formulation and storage of *Arthrobacter aurescens* strain TC1 as a bioremediation tool for terbuthylazine contaminated soils: Efficacy on abatement of aquatic ecotoxicity. *Sci. Total Environ.* **2019**, *668*, 714–722. [CrossRef]
26. Ofaim, S.; Zarecki, R.; Porob, S.; Gat, D.; Freilich, S. Genome-scale reconstruction of *Paenarthrobacter aurescens* TC1 metabolic model towards the study of atrazine bioremediation. *Sci. Rep.* **2020**, *10*, 13019. [CrossRef]
27. Saitou, N. The neighbor-joining methods: A new method for reconstructing phylogenetic trees. *Mol. Biol. Evol.* **1987**, *4*, 406–425.
28. Mongodin, E.F.; Shapir, N.; Daugherty, S.C.; Deboy, R.T.; Emerson, J.B.; Shvartzbeyn, A.; Radune, D.; Vamathevan, J.; Riggs, F.; Grinberg, V.; et al. Secrets of Soil Survival Revealed by the Genome Sequence of *Arthrobacter aurescens* TC1. *PLoS Genet.* **2007**, *2*, e214. [CrossRef]
29. Deutch, C.E. L-Proline catabolism by the high G+C Gram-positive bacterium *Paenarthrobacter aurescens* strain TC1. *Antonie van Leeuwenhoek* **2019**, *112*, 237–251. [CrossRef]
30. Schütte, M.; Fetzner, S. EstA from *Arthrobacter nitroguajacolicus* Rü61a, a thermo- and solvent-tolerant carboxylesterase related to class C beta-lactamases. *Curr. Microbiol.* **2007**, *54*, 230–236. [CrossRef]
31. Ryu, B.H.; Ngo, T.D.; Yoo, W.; Lee, S.; Kim, B.Y.; Lee, E.; Kim, K.K.; Kim, T.D.J.R. Biochemical and Structural Analysis of a Novel Esterase from *Caulobacter crescentus* related to Penicillin-Binding Protein (PBP). *Sci. Rep.* **2016**, *6*, 37978. [CrossRef] [PubMed]
32. Gao, X.; Mao, X.; Lu, P.; Secundo, F.; Sun, J.J.C. Cloning, Expression, and Characterization of a Novel Thermostable and Alkaline-stable Esterase from *Stenotrophomonas maltophilia* OUC_Est10 Catalytically Active in Organic Solvents. *Catalysts* **2019**, *9*, 401. [CrossRef]
33. Wagner, U.G.; Dimaio, F.; Kolkenbrock, S.; Fetzner, S. Crystal structure analysis of EstA from *Arthrobacter* sp. Rue61a—An insight into catalytic promiscuity. *FEBS Lett.* **2014**, *588*, 1154–1160. [CrossRef] [PubMed]
34. Farberg, A.M.; Hart, W.K.; Johnson, R.J.J.B.; Reports, B. The unusual substrate specificity of a virulence associated serine hydrolase from the highly toxic bacterium, *Francisella tularensis*. *Biochem. Biophys. Rep.* **2016**, *7*, 415–422. [CrossRef] [PubMed]
35. Kim, Y.; Zhou, M.; Gu, M.; Anderson, W.F.; Joachimiak, A. Crystal Structure of Beta-Lactamase/D-Alanine Carboxypeptidase from *Chromobacterium violaceum*. *Acta Crystallogr.* **1998**, *54*, 657–658.
36. Trott, O.; Olson, A.J. AutoDock Vina: Improving the speed and accuracy of docking with a new scoring function, efficient optimization, and multithreading. *J. Comput. Chem.* **2009**, *31*, 72–82. [CrossRef]
37. Gao, M.; Li, Y.; Xue, X. Stable Plastid Transformation for High-Level Recombinant Protein Expression: Promises and Challenges. *Biomed Res. Int.* **2013**, *2012*, 158232. [CrossRef]
38. Hao, H.; Yang, W.; Guocheng, D.U.; Zhen, K. Research progress in microbial expression systems for recombinant protein production. *Biotechnol. Bus.* **2009**, *74*, 250–256.
39. Zhang, S.; Wang, M.; Han, M.; Ma, R.; Chen, Q.; Gao, J. Optimization of Fermentation and Induction Conditions of Recombinant *E. coli* BL21(DE3)/pET30a(+)hrpNEcc. *China Biotechnol.* **2019**, *29*, 44–49.
40. Wilms, B.; Wiese, A.; Syldatk, C.; Mattes, R.; Pietzsch, M. Cloning, nucleotide sequence and expression of a new L-N-carbamoylase gene from *Arthrobacter aurescens* DSM 3747 in *E. coli*. *J. Biotechnol.* **1999**, *68*, 101–113. [CrossRef]
41. Zhou, X.; Wang, Q.; Wang, Z.; Xie, S. Nitrogen impacts on atrazine-degrading *Arthrobacter* strain and bacterial community structure in soil microcosms. *Environ. Sci. Pollut. Res.* **2013**, *20*, 2484–2491. [CrossRef] [PubMed]
42. Wilhelm, S.; Gdynia, A.; Tielen, P.; Rosenau, F.; Jaeger, K.E. The Autotransporter Esterase EstA of *Pseudomonas aeruginosa* Is Required for Rhamnolipid Production, Cell Motility, and Biofilm Formation. *J. Bacteriol.* **2007**, *17*, 13–25. [CrossRef] [PubMed]
43. Bradford, M.M. A rapid and sensitive method for the quantitation of microgram quantities of protein utilizing the principle of protein-dye binding. *Anal. Biochem.* **1976**, *72*, 248–254. [CrossRef]
44. Faulds, C.B.; Williamson, G. Purification and characterization of a ferulic acid esterase (FAE-III) from *Aspergillus niger*: Specificity for the phenolic moiety and binding to microcrystalline cellulose. *Microbiology* **1994**, *140*, 779–787. [CrossRef]